Cancer type-SLCO1B3 promotes epithelial-mesenchymal transition resulting in the tumour progression of non-small cell lung cancer

HIROAKI HASE[1], MASAYA AOKI[2], KENTARO MATSUMOTO[1], SHUICHI NAKAI[1], TOSHIYUKI NAGATA[2], AYA TAKEDA[2], KAZUHIRO UEDA[2], KENTARO MINAMI[3], KAORI KITAE[1], KENTARO JINGUSHI[1], YUKO UEDA[1], MASATATSU YAMAMOTO[3], TATSUHIKO FURUKAWA[3], MASAMI SATO[2] and KAZUTAKE TSUJIKAWA[1]

[1]Laboratory of Molecular and Cellular Physiology, Graduate School of Pharmaceutical Sciences, Osaka University, Suita, Osaka 565-0871; Departments of [2]General Thoracic Surgery, [3]Molecular Oncology, Graduate School of Medical and Dental Sciences, Kagoshima University, Kagoshima, Kagoshima 890-8544, Japan

Received July 17, 2020; Accepted September 25, 2020

DOI: 10.3892/or.2020.7839

Abstract. Non-small cell lung cancer (NSCLC) is one of the most common histologically defined subtypes of lung cancer. To identify a promising molecular target for NSCLC therapy, we performed gene expression analysis at the exon level using postoperative specimens of NSCLC patients. Exon array and real-time PCR analyses revealed that an alternative splicing variant of solute carrier organic anion transporter family member 1B3 (SLCO1B3) called cancer type-SLCO1B3 (Ct-SLCO1B3) was significantly upregulated in the NSCLC samples. SLCO1B3 expressed in the liver [liver type (Lt)-SLCO1B3] was found to be localised in the cell membrane, whereas Ct-SLCO1B3 was detected in the cytoplasm of NSCLC cells. RNAi-mediated knockdown of Ct-SLCO1B3 inhibited *in vitro* anchorage-independent cell growth, cell migration, and *in vivo* tumour growth of A549 cells. Overexpression of Ct-SLCO1B3 but not Lt-SLCO1B3 upregulated anchorage-independent cell growth and cell migration of NCI-H23 cells. Mechanistically, Ct-SLCO1B3 was found to regulate the expression of epithelial-mesenchymal transition (EMT)-related genes. The upregulation of E-cadherin was discovered to be especially pivotal to phenotypes of Ct-SLCO1B3-suppressed A549 cells. These findings suggest that Ct-SLCO1B3 functions as a tumour-promoting factor via regulating EMT-related factors in NSCLC.

Correspondence to: Dr Hiroaki Hase, Laboratory of Molecular and Cellular Physiology, Graduate School of Pharmaceutical Sciences, Osaka University, 1-6 Yamadaoka, Suita, Osaka 565-0871, Japan
E-mail: hase-h@phs.osaka-u.ac.jp

Key words: SLCO1B3, non-small cell lung cancer, epithelial-mesenchymal transition, E-cadherin, anchorage-independent cell growth, migration, invasion

Introduction

Lung cancer is one of the most common cancers leading to patient death (1). Non-small cell lung cancer (NSCLC) is the most frequent subtype of lung cancer, and the predicted 5-year survival rate remains poor despite recent therapeutic advances (2,3). Although molecular-targeted drugs have been developed against specific molecules in NSCLC, including epidermal growth factor receptor (EGFR) and anaplastic lymphoma kinase, there are many NSCLC patients who do not receive treatment with these drugs (4-6). Therefore, it is necessary to clarify further the molecular mechanisms involved in NSCLC tumourigenesis and progression for improving the therapeutic strategies for NSCLC.

Solute carrier organic anion transporter family member 1B3 (SLCO1B3) is a member of the organic anion transporting polypeptide (OATP/SLCO) superfamily. SLCO1B3 plays a role in the uptake of a variety of endogenous compounds (e.g., bile acids, cholecystokinin, conjugated steroids, and thyroid hormones) as well as clinically relevant drugs (7-11). SLCO1B3 was initially considered as a liver-specific transporter; however, recent research has demonstrated that this gene is transcribed at low levels in several extrahepatic tissues (10). Previous studies have revealed that some cancerous tissues and cells (e.g. colon, lung, and pancreatic cancers) express an alternative splicing form of SLCO1B3 [cancer type-SLCO1B3 (Ct-SLCO1B3)] (12-14). Since Ct-SLCO1B3 mRNA is transcribed from within intron 2 of the *SLCO1B3* gene, it lacks a part of the N-terminal coding region of full-length SLCO1B3. The function of Ct-SLCO1B3 remains largely unknown in cancer.

In the present study, we detected significantly upregulated Ct-SLCO1B3 in NSCLC tissues compared to that noted in normal lung tissues. Ct-SLCO1B3 contributed to anchorage-independent cell growth, cell migration, and tumour growth in NSCLC cells, whereas Lt-SLCO1B3 did not show these phenotypes. Moreover, we found that Ct-SLCO1B3 is involved in maintaining the expression of epithelial-mesenchymal transition (EMT)-related genes.

Reductions in anchorage-independent cell growth and migration by Ct-SLCO1B3 knockdown were mediated by the upregulation of E-cadherin. To the best of our knowledge, this is the first study to show that Ct-SLCO1B3 promotes NSCLC progression via regulation of EMT.

Materials and methods

NSCLC clinical samples and NSCLC cell lines

Gene expression analysis in clinical specimens. Specimens of NSCLC tissues and adjacent noncancerous tissues were obtained from 101 patients who had undergone primary curative resection of lung tumours at Kagoshima University Hospital (Japan). Information concerning the clinical specimens from the NSCLC patients is shown in Table SI. This study was approved by the Ethics Committee of Kagoshima University Hospital. All patients signed informed consent prior to their inclusion in the study. The samples were stored immediately at -80˚C by immersing in RNAlater (Qiagen, Germany) 24 h prior to RNA extraction. mRNA was purified using an miRNeasy Mini kit (Qiagen). Real-time polymerase chain reaction (real-time PCR) analysis was conducted to validate Ct-SLCO1B3 expression in NSCLC using 101 matched paired specimens of NSCLC.

NSCLC cell lines. Human lung adenocarcinoma cell lines (A549, HLC-1, LC-2/ad, and RERF-LC-KJ) and human lung squamous cancer cell lines (EBC-1, LC-1F, LK-2, RERF-LC-AI, and Sq-1) were obtained from RIKEN Cell Bank (Japan). Human lung adenocarcinoma cell lines (NCI-H1650 NCI-H1975, NCI-H2228, II-18, PC-14, Calu-3, NCI-H1755, NCI-H1792, NCI-H1838, NCI-H23, and NCI-H1437) and human lung squamous cancer cell lines (NCI-H226 and NCI-H520) were obtained from the American Type Culture Collection.

Exon array analysis. Total RNA (100 ng) from 4 matched paired samples of NSCLC were subjected to cDNA synthesis by Ambion WT Expression kit (Thermo Fisher Scientific, Inc.). The obtained cDNA was fragmented and biotinylated by fragmentation using the GeneChip WT Terminal Labeling Kit (Affymetrix; Thermo Fisher Scientific, Inc.) and was hybridised to the GeneChip Human Exon 1.0 ST Array (Affymetrix; Thermo Fisher Scientific, Inc.) for 17 h. After hybridization, GeneChips were washed and stained with the GeneChip Hybridization Wash and Stain Kit (Affymetrix; Thermo Fisher Scientific, Inc.) using the Fluidics Station (Affymetrix; Thermo Fisher Scientific, Inc.), and the chips were scanned using the 3000 GeneChip Scanner. Gene Spring 12.1 (Agilent Technologies, Inc.) was used for data analysis.

Cell culture. RPMI-1640 medium (Wako Japan, for NCI-H23, HLC-1, LC-2/ad, RERF-LC-KJ, EBC-1, LC-1F, LK-2, RERF-LC-AI, and Sq-1) and DMEM (Wako, for A549, NCI-H1650 NCI-H1975, NCI-H2228, II-18, PC-14, Calu-3, NCI-H1755, NCI-H1792, NCI-H1838, NCI-H23, NCI-H1437, NCI-H226, and NCI-H520) supplemented with 10% fetal calf serum (FCS) and 100 mg/l kanamycin were used as cell culture media at 37˚C under a 5% CO_2 atmosphere.

Extraction of total RNAs and real-time PCR analysis. Total RNA was isolated using Trizol reagent (Invitrogen; Thermo Fisher Scientific, Inc.), and cDNA was synthesised using the Primescript RT reagent Kit (Takara Bio, Japan) according to the manufacturer's protocol. A light cycler (Roche Diagnostics, Switzerland) was used for real-time PCR analysis. The thermal cycling conditions were as follows: An initial step at 95˚C for 30 sec and 40 cycles at 95˚C for 15 sec, 58˚C for 30 sec (GAPDH) or 40 cycles at 95˚C for 15 sec, and 62˚C for 30 sec (Ct-SLCO1B3 exon 1*-3, SLCO1B3 exon 9-10). The primer sequences used for the gene amplification were as follows: Ct-SLCO1B3 exon 1*-3 forward primer, 5'-TTC CCTGGGGAGAGGGACATACA-3' and reverse primer, 5'-CCAGCAAGAGAAGAGGATATGTCA-3'; Ct-SLCO1B3 exon 9-10 forward primer, 5'-GTCCAGTCATTGGCTTTG CA-3' and reverse primer, 5'-CAACCCAACGAGAGTCCT TAGG-3'; GAPDH forward primer, 5'-CCATCACCATCT TCCAGGAG-3' and reverse primer 5'-AATGAGCCCCAG CCTTCTCC-3'. Extraction of total RNAs and real-time PCR analysis for Snail and Slug are outlined in Data S1.

RT-PCR analysis of full-length Ct-SLCO1B3 and Lt-SLCO1B3. Total RNA was isolated using the Trizol reagent (Invitrogen; Thermo Fisher Scientific, Inc.). The PrimeScript RT reagent Kit (Takara Bio) was used for the preparation of cDNA from 500 ng total RNA samples. The thermal cycling conditions were as follows: An initial step at 94˚C for 120 sec, 40 cycles at 94˚C for 30 sec, and 68˚C for 150 sec using Ct-SLCO1B3 or Lt-SLCO1B3 full-length primer as follows: Ct-SLCO1B3 forward primer, 5'-ATGGGATGGCTTGGCTTGG-3' and reverse primer, 5'-TTAGTTGGCAGCAGCATTGTCTTG-3'; Lt-SLCO1B3 forward primer, 5'-ATGGACCAACATCAA CATTTGAATAAAAC-3' and reverse primer 5'-ATGGGA TGGCTTGGCTTGG-3'.

Small interfering RNA (siRNA) transfection. siRNA duplexes used to downregulate Ct-SLCO1B3 mRNA (Ct-SLCO1B3 siRNA: ACGUUACUGAAUCUACAUGTT) and the negative control siRNA duplex (Control siRNA: AUCCGCGCG AUAGUACGUATT) were purchased from Gene Design Inc. (Japan). Stealth RNAi siRNAs used to downregulate E-cadherin mRNA (E-cadherin siRNA #1, ACACUGCCA ACUGGCUGGAGAUUAA and E-cadherin siRNA #2, GAGCACGUGAAGAACAGCACGUAUA) and the negative control Stealth RNAi siRNA duplex (the sequence has not been published) were purchased from Life Technologies. Ct-siRNAs of SLCO1B3 and E-cadherin were transfected at concentrations of 10 nM and the indicated concentrations, respectively, using Lipofectamine RNAiMAX (Invitrogen; Thermo Fisher Scientific, Inc.) in accordance with the manufacturer's protocol.

Western blotting. The whole-cell lysates were separated by sodium dodecyl sulphate (SDS)-polyacrylamide gel (10%) electrophoresis (PAGE) and then transferred to a polyvinylidene difluoride (Merck Millipore) membrane using XCell SureLock Mini-Cell and XCell II Blot Module (Invitrogen; Thermo Fisher Scientific, Inc.). The membranes were probed with specific antibodies and then incubated with horseradish peroxidase-conjugated antibodies against mouse

or rabbit immunoglobulin (Cell Signaling Technology, Inc.). Immunoreactive proteins were detected by treatment with a detection reagent (ECL Prime Western Blotting Detection Reagent, GE Healthcare). The ImageQuant LAS4000 Mini System (GE Healthcare) was used for chemiluminescence detection. The following antibodies were used for immunological analysis in this study: Polyclonal anti-β-actin antibodies (dilution 1:1,000; cat. no. sc-69879; Santa Cruz Biotechnology, Inc. USA), anti-E-cadherin (dilution 1:1,000; cat. no. 3195; Cell Signaling Technology, Inc.), Snail (dilution 1:1,000; cat. no. 3879; Cell Signaling Technology, Inc.), Slug (dilution 1:1,000; cat. no. 9585; Cell Signaling Technology, Inc.), TCF8/ZEB1 (dilution 1:1,000; cat. no. 3396; Cell Signaling Technology, Inc.), and vimentin antibodies (dilution 1:1,000; cat. no. 5741P; Cell Signaling Technology, Inc.).

Construction of Ct-SLCO1B3 and Lt-SLCO1B3 expression plasmids. cDNAs of Ct-SLCO1B3 and Lt-SLCO1B3 were amplified via PCR using total RNAs of A549 cells and normal liver cells, respectively. The primer sequences for gene amplification were as follows: Ct-SLCO1B3 forward primer, 5'-CCCTGAGATGGGATGGCTTGGCTTGG-3' and reverse primer, 5'-CCGGATCCGTTGGCAGCAGCATTGTCTTG-3'; Lt-SLCO1B3 forward primer, 5'-CCCTGAGAATGGACCAACATCAACATTTGAATAAAAC-3' and reverse primer 5'-CCGGATCCGTTGGCAGCAGCATTGTCTTG-3'. The gel-purified PCR products ligated into the pT7-blue vector (Merck Millipore) using the Perfectly Blunt Cloning Kit (Merck Millipore) were transformed into *E. coli* DH5α (Takara Bio). The plasmid was purified from DH5α and treated with a restriction enzyme for insertion into the pcDNA3.0 vector (Invitrogen; Thermo Fisher Scientific, Inc.) using Ligation High (Toyobo).

Anchorage-independent cell growth assay. siRNA and Stealth RNAi siRNA transfected A549 cells were suspended in FCeM-D (Nissan Chemical) with 10% FCS and were seeded in a HydroCell 96-well plate (CellSeed) (1,000 cells/well) 48 h after transfection. NCI-H23 cells were seeded in a 96-well plate (4,000 cells/well). Two hours after incubation with the WST-1 reagent (Dojindo) at 37˚C in 5% CO_2, the optical density was read at a wavelength of 450/630 nm (Ex/Em).

Wound healing assay. Cell migration was examined by the wound healing assay. A549 ($6x10^4$ cells/well) and NCI-H23 ($1x10^5$ cells/well) cells were seeded in a 48-well plate 48 h after transfection. A wound was created in a monolayer of about 80-90% confluent A549 or NCI-H23 cells using a sterile 1-ml pipette tip. Cell migration images were recorded at 0, 6, 12, 24, 36, and 48 (only A549) h with an Olympus IX71 fluorescence microscope (Olympus) at a x100 magnification.

siRNA administration in an in vivo xenograft model. A549 cells were suspended in an equal volume of Matrigel Matrix High Concentration (Corning, Inc.) and injected subcutaneously into 7-week-old male BALB/c nu-nu mice. Eleven days after the injection, 14 tumour-bearing mice were divided into two groups. Tumour size was measured on days 11, 15, 18, 22, 25, 29 and 32 after tumour cell injection, and siRNA was administered on days 12, 19 and 26 after the injection. The siRNA solution was prepared with AteloGene Local Use 'Quick Gelation' (Koken) as a carrier, and 4 nmol/mouse/150 μl was injected. On day 32 after tumour cell injection, mice were sacrificed, tumours were enucleated from each mouse, and the tumour weight was measured.

Statistics. Results are expressed as the mean ± standard deviation of the mean (SD). Differences between values were statistically analysed using a Student's t-test or one-way ANOVA with Bonferroni post-hoc test (GraphPad Prism 5.0, GraphPad Software). A P-value <0.05 was considered to indicate statistical significance.

Results

Ct-SLCO1B3 is expressed in NSCLC. To explore the alternative splicing signature in NSCLC, we performed an exon array analysis using four matched pairs of postoperative specimens of NSCLC patients. We focused on SLCO1B3 since the exon usage for this gene is different between NSCLC tissues and the adjacent normal tissues. As shown in Fig. 1A, we found a high probe set intensity of SLCO1B3 exons 3-15 in only 2 samples from cancerous tissues of NSCLC patients (cancers 2 and 3). Interestingly, the probe intensity of SLCO1B exon 2 in these two samples was as low as that in all the other samples, including the adjacent normal lung tissues. This result suggested that SLCO1B3 in the two samples was transcribed with its 5'-end missing. The expression of SLCO1B3 lacking exon 2 (Ct-SLCO1B3) has been detected in some cancers (Fig. S1A). Therefore, we amplified the gene fragment in the two samples using primers designed around SLCO1B3 exons 1 and 3 and confirmed the deletion of SLCO1B3 exon 2 by sequencing. Then, we determined Ct-SLCO1B3 expression in 101-matched paired NSCLC specimens by real-time PCR using a specific primer set as described above. As shown in Fig. 1B, Ct-SLCO1B3 was detected in 26 specimens of NSCLC tissues but not in adjacent normal tissue specimens. Ct-SLCO1B3 expression in NSCLC was independent of EGFR mutation, patient sex, and NSCLC subtype and was also detected in specimens with stage IA LSCLC cancer (Fig. S2). Immunohistochemical examination showed that Ct-SLCO1B3 was localised to the cytoplasm of NSCLC cells, but no signal was found in normal lung tissue (Fig. 1C). Lt-SLCO1B was localised in the cell membrane of hepatocytes, as described previously (Fig. S1B) (13).

Ct-SLCO1B3 plays roles in anchorage-independent cell growth and migration of A549 cells. To investigate Ct-SLCO1B3 function in NSCLC cells, we first evaluated Ct-SLCO1B3 mRNA expression levels in 22 lung cancer cell lines. Among the lung cancer cell lines, Ct-SLCO1B3 mRNA expression was predominant in the adenocarcinoma cell lines (Fig. S3). We selected A549 and NCI-H23 cells based on expression levels of Ct-SLCO1B3 and transfection efficiency for subsequent experiments. To assess the knockdown efficiency of Ct-SLCO1B3 siRNAs, real-time PCR was conducted. As shown in Fig. 2A, the expression level of Ct-SLCO1B3 mRNA was sufficiently reduced by Ct-SLCO1B3 siRNA in the A549 cells. To investigate the potential function of Ct-SLCO1B3, we examined the effect of Ct-SLCO1B3 siRNA on anchorage-independent

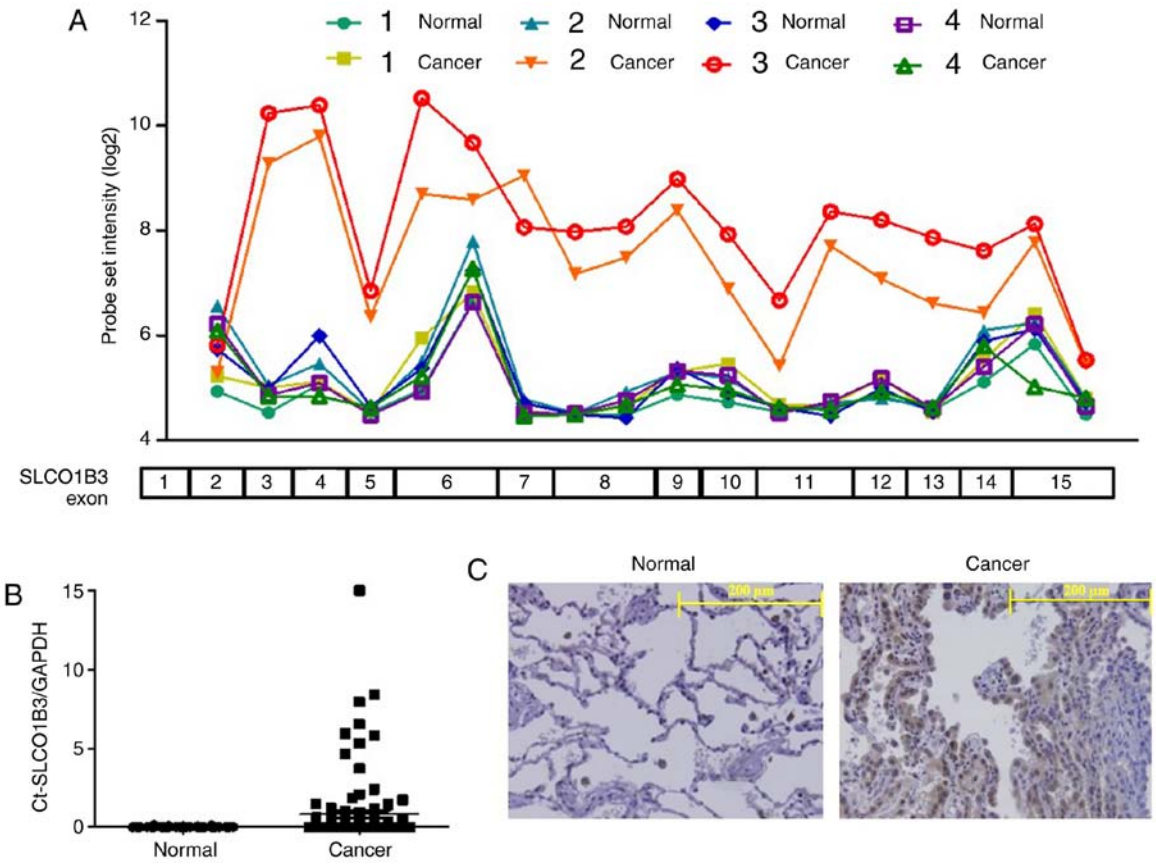

Figure 1. Ct-SLCO1B3 is highly expressed in NSCLC clinical specimens. (A) Exon array was performed in four matched pairs of clinical specimens of NSCLC. 'Normal' and 'Cancer' represent mean data from adjacent normal and cancer tissues, respectively. (B) mRNAs of Ct-SLCO1B3 and GAPDH were quantified by real-time PCR in 101 matched tumour-normal tissue pairs. (C) Ct-SLCO1B3 localization was examined by immunohistochemistry using an anti-SLCO1B3 antibody. NSCLC, non-small cell lung cancer; Ct-SLCO1B3, cancer type-solute carrier organic anion transporter family member 1B3.

cell growth and migration in A549 cells. Ct-SLCO1B3 siRNA significantly suppressed anchorage-independent cell growth (Fig. 2B) and decreased the migration ability (Figs. 2C and S4) of the A549 cells.

Next, we carried out overexpression experiments of Ct-SLCO1B3 and Lt-SLCO1B3 using NCI-H23 cells with a deficient expression of Ct-SLCO1B3. Plasmid vector pcDNA3.0 containing either Lt-SLCO1B3 or Ct-SLCO1B3 cDNA was transfected into NCI-H23 cells, and similar expression levels of each SLCO1B3 mRNA were confirmed by real-time PCR using specific primer sets of Lt-SLCO1B3 and Ct-SLCO1B3 (Fig. 2D and E). Then, we investigated the effect of Lt-SLCO1B3 or Ct-SLCO1B3 overexpression on anchorage-independent cell growth and migration. Overexpression of Ct-SLCO1B3 but not Lt-SLCO1B3 significantly increased anchorage-independent cell growth and migration (Fig. 2F and G). These results indicated that Ct-SLCO1B3 and Lt-SLCO1B3 exhibit different biological functions, and only Ct-SLCO1B3 may contribute to NSCLC development.

Ct-SLCO1B3 regulates anchorage-independent cell growth and cell migration via EMT-related gene expression. In siRNA transfection experiments, we observed morphological changes in Ct-SLCO1B3-knockdown A549 cells, which resembled epithelial cells with tight cell-cell interaction (Fig. 3A). From this observation, we assumed that Ct-SLCO1B3 regulates EMT. Since EMT is a crucial step in cancer progression, that facilitates cancer cells to lose cell polarity and cell-to-cell adhesion to gain migratory and invasive properties (15-17), we investigated the mRNA (Fig. S5A) and protein (Fig. 3B) expression of EMT-related factors. An epithelial cell marker, E-cadherin, was upregulated in Ct-SLCO1B3-knockdown A549 cells. On the other hand, suppression of Ct-SLCO1B3 expression reduced the expression of mesenchymal related genes, Snail, Slug, TCF8/ZEB1, and vimentin. Moreover, prominent E-cadherin localization in the cell-cell contact region was observed in Ct-SLCO1B3 siRNA-transfected A549 cells (Fig. S5B). These results suggest that Ct-SLCO1B3 facilitates EMT in NSCLC cells. To demonstrate that phenotype induction by Ct-SLCO1B3 knockdown occurred via the upregulation of E-cadherin, we performed Ct-SLCO1B3 and E-cadherin double knockdown experiments. Upregulation of E-cadherin by Ct-SLCO1B3 siRNA was diminished following transfection with two types of E-cadherin stealth siRNAs (Fig. 3C). Suppression of anchorage-independent cell growth and migration by Ct-SLCO1B3 siRNAs was reversed by transfection of both E-cadherin stealth siRNAs (Fig. 3D and E). These experiments indicated that Ct-SLCO1B3 is related to EMT in NSCLC cells, and E-cadherin plays an important role in anchorage-independent cell growth and migration in Ct-SLCO1B3-knockdown A549 cells.

Ct-SLCO1B3 facilitates tumourigenesis in NSCLC xenograft model mice. Since anchorage-independent cancer

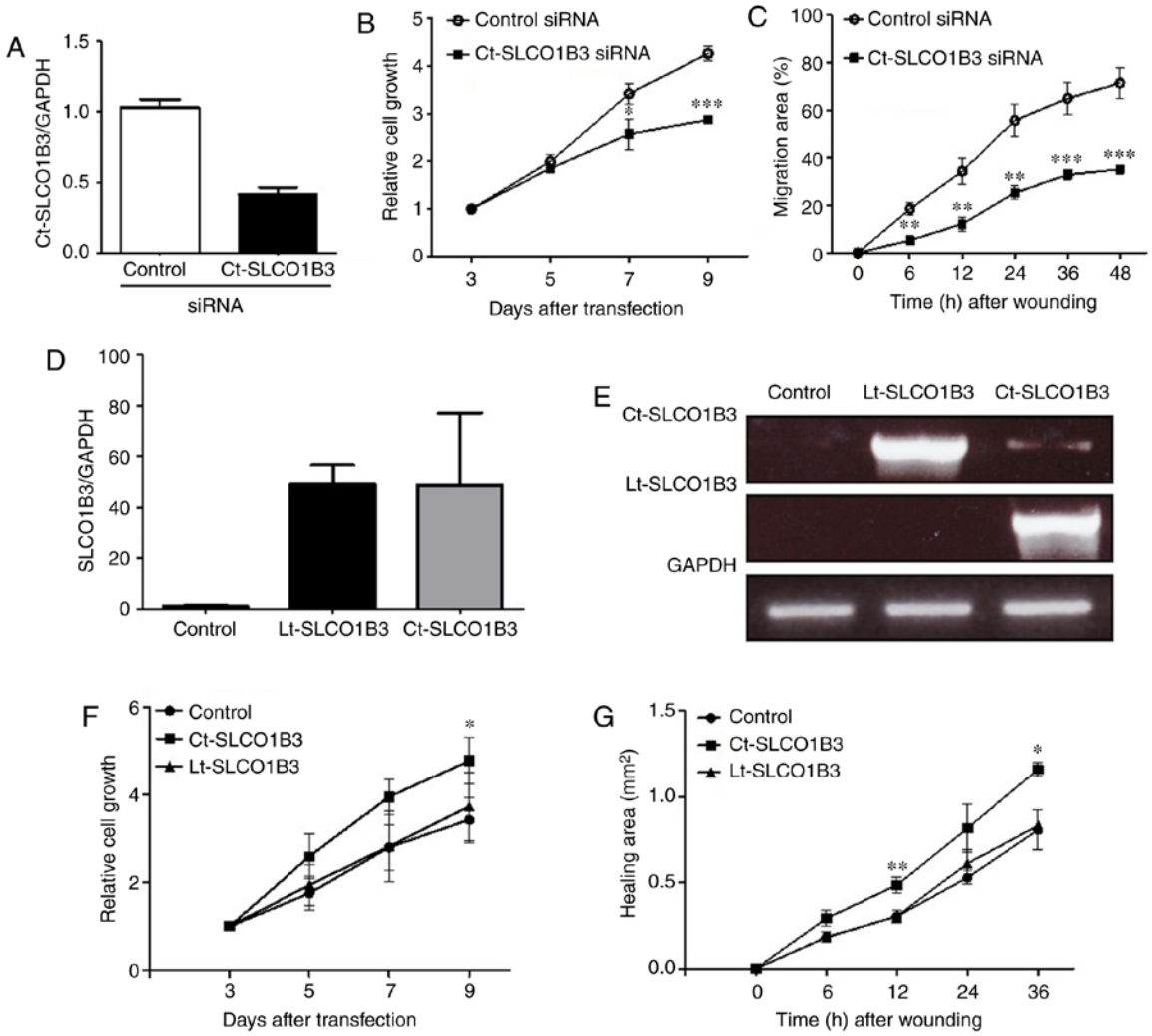

Figure 2. Ct-SLCO1B3 regulates anchorage-independent cell growth and migration. (A) A549 cells were transfected with control and Ct-SLCO1B3 siRNAs at 10 nM. mRNAs of Ct-SLCO1B3 and GAPDH were quantified by real-time PCR analysis. Scrambled siRNA was used as a control. Data are expressed as mean ± SD of three independent experiments. (B) Anchorage-independent A549 cell growth was examined from 3 to 9 days after siRNA transfection. (C) Confluent A549 cells were scratched and migration area was measured. Data are expressed as mean ± SD of triplicate experiments in (B) and (C). (D) NCI-H23 cells were transfected with Lt-SLCO1B3 or Ct-SLCO1B3 cDNAs containing pcDNA3.0 vectors. After G418 selection, the clone stably expressing Lt-SLCO1B3 or Ct-SLCO1B3 was selected. The mRNAs of SLCO1B3 and GAPDH were quantified by real-time PCR. pcDNA3.0 empty vector was used as a control. (E) PCR was performed to confirm the expression of a full-length of Lt-SLCO1B3 or Ct-SLCO1B3. Specific primer sets were utilised to determine full-length of Lt-SLCO1B3 or Ct-SLCO1B3 mRNA. Data are expressed as the mean ± SD of triplicate experiments, and the experiments were repeated 3 times with similar results. (F and G) pcDNA3.0 empty vector (control), Lt-SLCO1B3, and Ct-SLCO1B3 expression vectors were transfected in NCI-H23 cells. Anchorage-independent A549 cell growth was examined from 3 to 9 days after cell seeding (F) Confluent A549 cells were scratched, and the migration area was measured from 6 to 36 h after scratching (G). *P<0.05, **P<0.01 and ***P<0.005, compared to the control siRNA group; Student's t-test.

cell growth plays an important role in tumourigenesis, we supposed that Ct-SLCO1B3 contributes to tumour growth *in vivo*. To elucidate that Ct-SLCO1B3 regulates tumour formation *in vivo*, we established a xenograft model by subcutaneous injection of A549 cells in nude mice. After tumour formation was confirmed, we administered control or Ct-SLCO1B3 siRNAs subcutaneously for 7 days. Tumour volume measurement was performed after tumour volumes reached approximately 200 mm^3. As shown in Fig. 4A, Ct-SLCO1B3 siRNA significantly decreased tumour volume after 29 days of its administration. On day 32, formed tumours were resected and imaged (Fig. 4B). There was a reduction in tumour weight (Fig. 4C) as well as Ct-SLCO1B3 levels (Fig. 4D) in the group of mice treated with Ct-SLCO1B3 siRNA in comparison to the control siRNA group. These results demonstrated that Ct-SLCO1B3 is involved in tumour growth *in vivo*.

Discussion

To develop a novel drug for non-small cell lung cancer (NSCLC) therapy, it is crucial not only to identify a molecule with characteristic expression in cancer cells but also to understand how the molecule is associated with the development and progression of NSCLC. Sun *et al* reported that cancer type-solute carrier organic anion transporter family member 1B3 (Ct-SLCO1B3) expression is detected in fewer lung cancer specimens, including NSCLC and small cell carcinoma (14). In the present study, we examined Ct-SLCO1B3 expression in 101-matched paired NSCLC specimens, including its correlation with EGFR

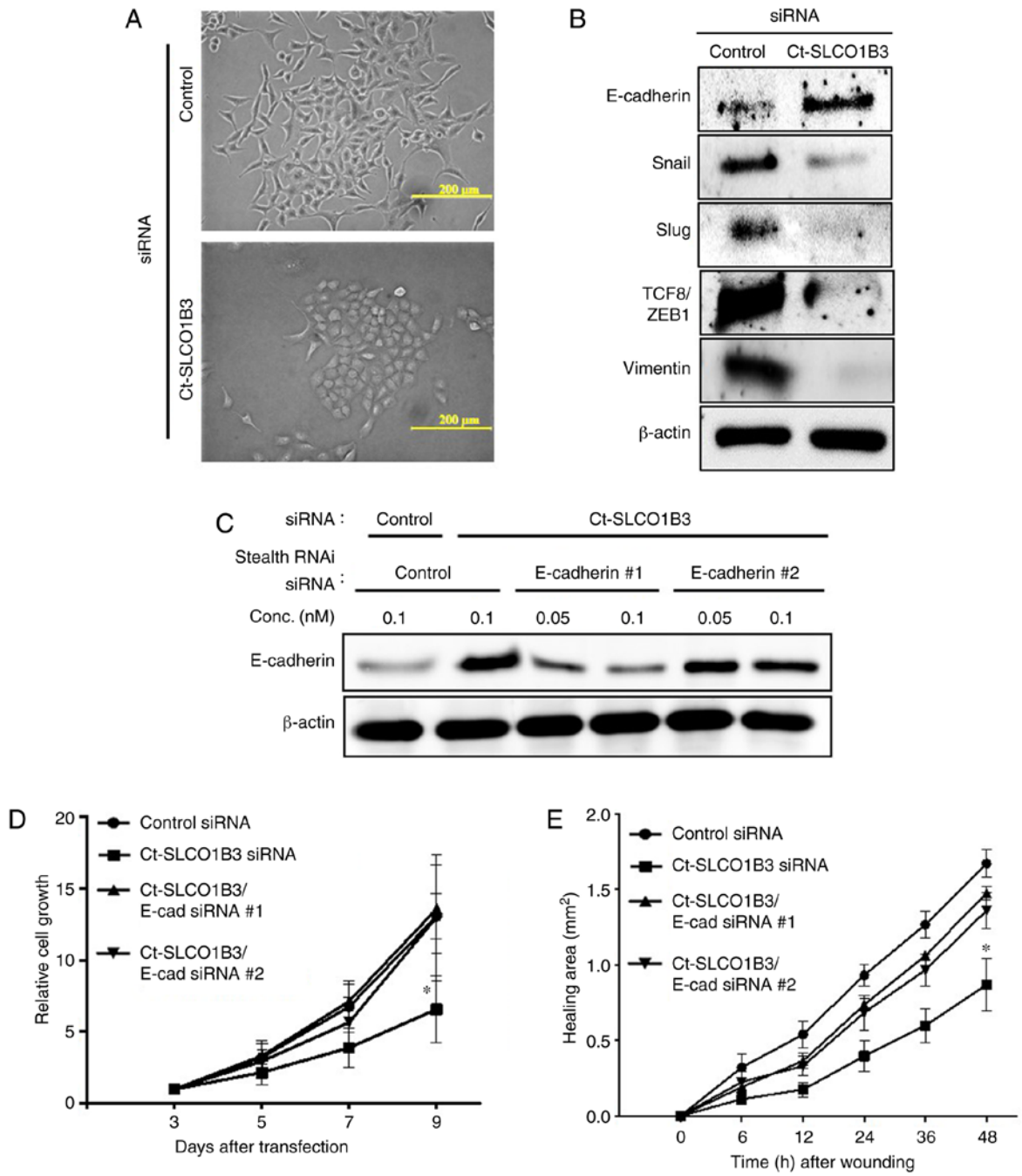

Figure 3. Phenotypes by Ct-SLC1B3 knockdown were mediated by the upregulation of E-cadherin expression in A549 cells. (A) A549 cells were transfected with control and Ct-SLCO1B3 siRNAs at 10 nM. Cell morphology was captured 48 h after transfection. (B) Protein levels of EMT-related markers were examined by western blot analysis. (C) A549 cells were co-transfected with Ct-SLCO1B3 siRNA and E-cadherin stealth RNAi siRNA at indicated concentrations. The protein expression of E-cadherin and β-actin were examined by western blot analysis. (D and E) A549 cells were co-transfected with Ct-SLCO1B3 siRNA and E-cadherin stealth RNAi siRNA at 10 and 0.1 nM, respectively. Anchorage-independent cell growth was examined from 3 to 9 days after transfection (D) Confluent A549 cells were scratched and healing area was measured from 6 to 48 h after scratching (E). Data are expresses as the mean ± SD of triplicate experiments. *P<0.05, compared to the control siRNA group; Student's t-test. Ct-SLCO1B3, cancer type-solute carrier organic anion transporter family member 1B3; ZEB1 (previously known as TCF8), zinc finger E-box binding homeobox 1.

mutation as well as pathological stages. Moreover, we clarified a molecular mechanism involving Ct-SLCO1B3 in the development and progression of NSCLC.

Loss of E-cadherin and upregulation of mesenchymal-related molecules such as vimentin, matrix metalloproteinase (MMP)-9, integrin-αvβ6, and N-cadherin are associated with poor clinical outcome in NSCLC (18,19). Moreover, it is well established that the state of epithelial-to-mesenchymal transition (EMT) affects the tumour response to various drugs, including epidermal growth factor receptor (EGFR) kinase inhibitors (20,21), indicating a crucial role of EMT in the progression and treatment of NSCLC. In this study, we showed that Ct-SLCO1B3 siRNA downregulated Snail, Slug, Zinc finger E-box binding homeobox 1 (ZEB1), and vimentin, and upregulated E-cadherin. Snail, Slug, and ZEB1 are known

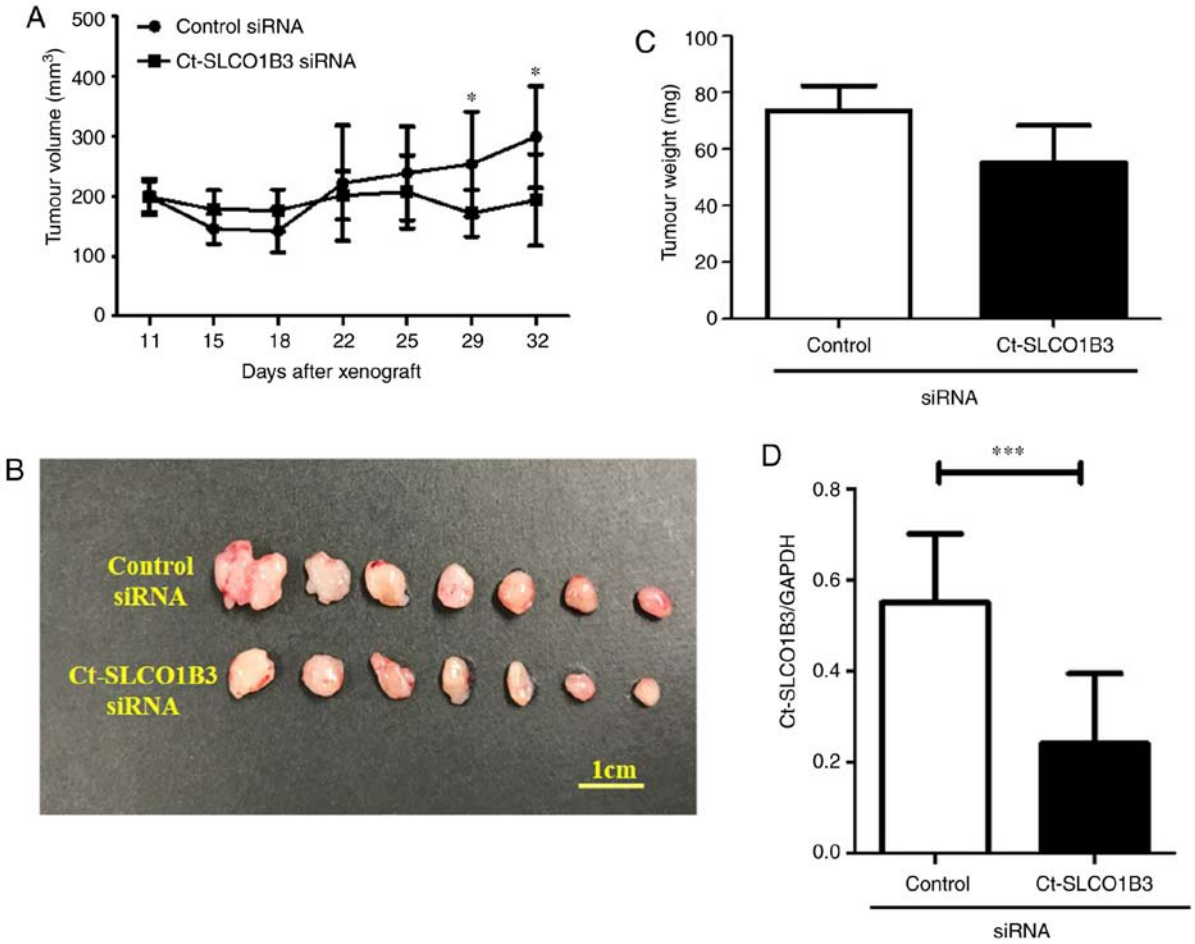

Figure 4. Ct-SLCO1B3 knockdown suppresses tumourigenesis *in vivo*. A549 cells were subcutaneously injected in nude mice with Matrigel. Control siRNA and Ct-SLCO1B3 siRNA were administered around a formed tumour with atelocollagen. (A) Tumour volume was measured at the indicated days. (B) Tumours were resected from mice 32 days after the xenograft and imaged. (C and D) Since the largest tumour from mice administered with a control siRNA was rejected by the Smirnov-Grubbs rejection test, the data represent the mean ± SD of six (control) or seven (Ct-SLCO1B3) mice. (C) Tumour weights in control or Ct-SLCO1B3-administered mice were measured. (D) Ct-SLCO1B3 and GAPDH mRNAs were quantified by real-time PCR analysis. *P<0.05 and ***P<0.005, compared with the siRNA control group; Student's t-test. Ct-SLCO1B3, cancer type-solute carrier organic anion transporter family member 1B3.

to be transcriptional regulators of E-cadherin. Therefore, Ct-SLCO1B3 knockdown was proposed to induce the expression of E-cadherin via the downregulation of these transcriptional regulators. Ct-SLCO1B3 and E-cadherin double knockdown experiments strongly supported that Ct-SLCO1B3 regulates E-cadherin expression in NSCLC. Ct-SLCO1B3 but not liver type (Lt)-SLCO1B3 facilitated the upregulation of anchorage-independent cell growth and cell migration in NSCLC cells by regulatory mechanisms. Research focusing on structural differences between Lt-SLCO1B3 and Ct-SLCO1B3 will lead to the elucidation of the detailed EMT-related molecular mechanisms in NSCLC. Furthermore, Ct-SLCO1B3 siRNA significantly decreased tumour growth in an *in vivo xenograft* mouse model experiment; however, whether Ct-SLCO1B3 regulates EMT via Snail, Slug, or ZEB1 *in vivo* remains unclear.

Lt-SLCO1B3 functions as a liver-specific organic anion transporter. However, it is not clear whether Ct-SLCO1B3 also functions as a transporter similar to Lt-SLCO1B3 in NSCLC. Additionally, Lt-SLCO1B3 is expressed on the cell membrane (22), while Ct-SLCO1B3 is localised in the cytoplasm of NSCLC cells. Based on this, we speculate that Ct-SLCO1B3, with its abnormal structure, may not exhibit similar transporter activity.

In conclusion, our present study showed that a subset of NSCLC patients express Ct-SLCO1B3, and Ct-SLCO1B3 significantly promoted anchorage-independent cell growth and cell migration through EMT induction in NSCLC cells. Moreover, *in vivo* tumour formation of NSCLC cells was suppressed by Ct-SLCO1B3 knockdown. These findings indicate that Ct-SLCO1B3 may be involved in the development and/or progression of NSCLC. Drugs specifically targeting Ct-SLCO1B3 could be a promising NSCLC therapy.

Acknowledgements

Not applicable.

Funding

This study was partially supported by Japan Agency for Medical Research and Development (AMED) (grant no. JP19lm0203007).

Availability of data and materials

The data sets generated in the present study are available from the corresponding author on reasonable request.

Authors' contributions

HH conceived and designed the study and participated in analysing the data. KMa and SN carried out the experiments, analysed the data, and drafted the manuscript. MA, TN, AT, KU, MS, KMi, MY and TF participated in providing and analysing the patient samples and supported the study. KK, KJ and YU participated in administrative, technical, or material support. KT developed a plan for whole this study, reviewed the draft manuscript and edited the manuscript. All authors read and approved the manuscript and agree to be accountable for all aspects of the research in ensuring that the accuracy or integrity of any part of the work are appropriately investigated and resolved.

Ethics approval and consent to participate

The study was approved by the Ethics Committee of Kagoshima University Hospital (Kogoshima, Japan). Written informed consent was obtained from each participant involved regarding the use of their tissues for research purposes.

Patient consent for publication

Not applicable.

Competing interests

The authors declare that they have no competing interests.

References

1. Siegel RL, Miller KD and Jemal A: Cancer statistics, 2016. CA Cancer J Clin 66: 7-30, 2016.
2. Ettinger DS, Wood DE, Aggarwal C, Aisner DL, Akerley W, Bauman JR, Bharat A, Bruno DS, Chang JY, Chirieac LR, *et al*: NCCN guidelines insights: Non-small cell lung cancer, version 1.2020. J Natl Compr Canc Netw 17: 1464-1472, 2019.
3. Chen Z, Fillmore CM, Hammerman PS, Kim CF and Wong KK: Non-small-cell lung cancers: A heterogeneous set of diseases. Nat Rev Cancer 14: 535-546, 2014.
4. Besse B, Adjei A, Baas P, Meldgaard P, Nicolson M, Paz-Ares L, Reck M, Smit EF, Syrigos K, Stahel R, *et al*: 2nd ESMO consensus conference on lung cancer: Non-small-cell lung cancer first-line/second and further lines of treatment in advanced disease. Ann Oncol 25: 1475-1484, 2014.
5. Pillai RN and Ramalingam SS: Advances in the diagnosis and treatment of non-small cell lung cancer. Mol Cancer Ther 13: 557-564, 2014.
6. Rolfo C, Giovannetti E, Hong DS, Bivona T, Raez LE, Bronte G, Buffoni L, Reguart N, Santos ES, Germonpre P, *et al*: Novel therapeutic strategies for patients with NSCLC that do not respond to treatment with EGFR inhibitors. Cancer Treat Rev 40: 990-1004, 2014.
7. Hagenbuch B and Meier PJ: The superfamily of organic anion transporting polypeptides. Biochim Biophys Acta 1609: 1-18, 2003.
8. Abe T, Unno M, Onogawa T, Tokui T, Kondo TN, Nakagomi R, Adachi H, Fujiwara K, Okabe M, Suzuki T, *et al*: LST-2, a human liver-specific organic anion transporter, determines methotrexate sensitivity in gastrointestinal cancers. Gastroenterology 120: 1689-1699, 2001.
9. Hagenbuch B and Meier PJ: Organic anion transporting polypeptides of the OATP/SLC21 family: Phylogenetic classification as OATP/SLCO superfamily, new nomenclature and molecular/functional properties. Pflugers Arch 447: 653-665, 2004.
10. Obaidat A, Roth M and Hagenbuch B: The expression and function of organic anion transporting polypeptides in normal tissues and in cancer. Annu Rev Pharmacol Toxicol 52: 135-151, 2012.
11. Yamaguchi H, Okada M, Akitaya S, Ohara H, Mikkaichi T, Ishikawa H, Sato M, Matsuura M, Saga T, Unno M, *et al*: Transport of fluorescent chenodeoxycholic acid via the human organic anion transporters OATP1B1 and OATP1B3. J Lipid Res 47: 1196-1202, 2006.
12. Nagai M, Furihata T, Matsumoto S, Ishii S, Motohashi S, Yoshino I, Ugajin M, Miyajima A, Matsumoto S and Chiba K: Identification of a new organic anion transporting polypeptide 1B3 mRNA isoform primarily expressed in human cancerous tissues and cells. Biochem Biophys Res Commun 418: 818-823, 2012.
13. Thakkar N, Kim K, Jang ER, Han S, Kim K, Kim D, Merchant N, Lockhart AC and Lee W: A cancer-specific variant of the SLCO1B3 gene encodes a novel human organic anion transporting polypeptide 1B3 (OATP1B3) localized mainly in the cytoplasm of colon and pancreatic cancer cells. Mol Pharm 10: 406-416, 2013.
14. Sun Y, Furihata T, Ishii S, Nagai M, Harada M, Shimozato O, Kamijo T, Motohashi S, Yoshino I, Kamiichi A, *et al*: Unique expression features of cancer-type organic anion transporting polypeptide 1B3 mRNA expression in human colon and lung cancers. Clin Transl Med 3: 37, 2014.
15. Thiery JP: Epithelial-mesenchymal transitions in tumour progression. Nat Rev Cancer 2: 442-454, 2002.
16. De Craene B and Berx G. Regulatory networks defining EMT during cancer initiation and progression. Nat Rev Cancer 13: 97-110, 2013.
17. Lamouille S, Xu J and Derynck R: Molecular mechanisms of epithelial-mesenchymal transition. Nat Rev Mol Cell Biol 15: 178-196, 2014.
18. Prudkin L, Liu DD, Ozburn NC, Sun M, Behrens C, Tang X, Brown KC, Bekele BN, Moran C, Moran C and Wistuba II: Epithelial-to-mesenchymal transition in the development and progression of adenocarcinoma and squamous cell carcinoma of the lung. Mod Pathol 22: 668-678, 2009.
19. Liu D, Huang C, Kameyama K, Hayashi E, Yamauchi A, Kobayashi S and Yokomise H: E-Cadherin expression associated with differentiation and prognosis in patients with non-small cell lung cancer. Ann Thorac Surg 71: 949-955, 2001.
20. Thomson S, Buck E, Petti F, Griffin G, Brown E, Ramnarine N, Iwata KK, Gibson N and Haley JD: Epithelial to mesenchymal transition is a determinant of sensitivity of non-small-cell lung carcinoma cell lines and xenografts to epidermal growth factor receptor inhibition. Cancer Res 65: 9455-9462, 2005.
21. Rho JK, Choi YJ, Lee JK, Ryoo BY, Na II, Yang SH, Kim CH and Lee JC: Epithelial to mesenchymal transition derived from repeated exposure to gefitinib determines the sensitivity to EGFR inhibitors in A549, a non-small cell lung cancer cell line. Lung Cancer 63: 219-226, 2009.
22. Chun SE, Thakkar N, Oh Y, Park JE, Han S, Ryoo G, Hahn H, Maeng SH, Lim YR, Han BW and Lee W: The N-terminal region of organic anion transporting polypeptide 1B3 (OATP1B3) plays an essential role in regulating its plasma membrane trafficking. Biochem Pharmacol 131: 98-105, 2017.